

# PCCP

Accepted Manuscript



This is an *Accepted Manuscript*, which has been through the Royal Society of Chemistry peer review process and has been accepted for publication.

*Accepted Manuscripts* are published online shortly after acceptance, before technical editing, formatting and proof reading. Using this free service, authors can make their results available to the community, in citable form, before we publish the edited article. We will replace this *Accepted Manuscript* with the edited and formatted *Advance Article* as soon as it is available.

You can find more information about *Accepted Manuscripts* in the [Information for Authors](#).

Please note that technical editing may introduce minor changes to the text and/or graphics, which may alter content. The journal's standard [Terms & Conditions](#) and the [Ethical guidelines](#) still apply. In no event shall the Royal Society of Chemistry be held responsible for any errors or omissions in this *Accepted Manuscript* or any consequences arising from the use of any information it contains.

# Metastable behavior of Noble Gas inserted Tin and Lead Fluorides

Sudip Pan,<sup>1</sup> Ashutosh Gupta,<sup>2</sup> Subhajit Mandal,<sup>1</sup> Diego Moreno,<sup>3</sup> Gabriel Merino,<sup>\*,3</sup> and  
Pratim K. Chattaraj.<sup>\*,1</sup>

<sup>1</sup>*Department of Chemistry and Centre for Theoretical Studies,  
Indian Institute of Technology, Kharagpur, 721302, India.*

<sup>2</sup>*Department of Chemistry, Udai Pratap Autonomous College,  
Varanasi, Uttar Pradesh, 221002 India.*

<sup>3</sup>*Departamento de Física Aplicada, Centro de Investigación y de Estudios  
Avanzados Unidad Mérida. km 6 Antigua carretera a Progreso. Apdo. Postal 73,  
Cordemex, 97310, Mérida, Yuc., México.*

\* Corresponding authors: [gmerino@mda.cinvestav.mx](mailto:gmerino@mda.cinvestav.mx),  
[pkc@chem.iitkgp.ernet.in](mailto:pkc@chem.iitkgp.ernet.in)

**Abstract**

*Ab initio* computations are carried out to explore the structure and stability of FNgEF<sub>3</sub> and FNgEF (E = Sn, Pb; Ng = Kr-Rn) compounds. They are the first reported systems to possess Ng-Sn and Ng-Pb bonds. Except FKrEF<sub>3</sub>, the dissociations of FNgSnF<sub>3</sub> and FNgEF producing Ng and SnF<sub>4</sub> or EF<sub>2</sub> are only exergonic in nature at room temperature whereas FNgPbF<sub>3</sub> has thermochemical instability with respect to two two-body dissociation channels. However, they are kinetically stable having positive activation barriers (ranging from 2.2 to 49.9 kcal/mol) with respect to those dissociations. The kinetic stability gradually improves in moving from Kr to Rn analogues. The remaining possible dissociation channels for these compounds are found to be endergonic in nature. The nature of bonding is analyzed by natural bond order, electron density, and energy decomposition analyses. Particularly, natural population analysis reveals that they are best represented as F<sup>-</sup>(NgEF<sub>3</sub>)<sup>+</sup> and F<sup>-</sup>(NgEF)<sup>+</sup>. All the Xe/Rn-E bonds in FNgEF<sub>3</sub> and FNgEF are covalent in nature.

**Keywords:** *Ab initio* study, dissociation channels, kinetic stability, natural population analysis, electron density analysis, energy decomposition analysis

## Introduction

For a long time, chemists had been facing a challenge to make noble gas (Ng) as a bonding partner due to their very unreactive nature. Earlier attempts to synthesize<sup>1</sup> noble gas compounds on the basis of theoretical predictions<sup>2</sup> were not convincing. Later, Pauling on the basis of ionic radii of different Ng atoms predicted the existence of  $\text{Ag}_4\text{XeO}_6$ ,  $\text{AgH}_3\text{XeO}_6$ ,  $\text{KrF}_6$  and  $\text{XeF}_6$ .<sup>3</sup> Experimental efforts towards the achievement of these predictions were found to be challenging,<sup>4</sup> and it was only in 1962 when Bartlett<sup>5</sup> and others<sup>6-8</sup> announced the preparation of first noble gas compounds. Since then several researchers have either experimentally detected<sup>9-13</sup> or theoretically predicted a large number of Ng compounds.<sup>14-20</sup> As a result, more than 500 such compounds have already been detected,<sup>21</sup> and literature contains excellent review articles<sup>22-25</sup> on this subject as well. Interest in Ng-C compounds grew with the reporting of first Xe-C bond in  $\text{XeCH}_3^+$  by Holtz and Beauchamp<sup>26</sup> in 1971 followed by the reporting of  $\text{Xe}(\text{CF}_3)_2$  in 1979 and pentafluorophenylxenon cation in 1989.<sup>27</sup> Subsequently there has been a plethora of work reported in the field of Xe-C containing organoxenon derivatives.<sup>28</sup> Under cryogenic environment, different Xe-C containing compounds such as  $\text{HXeCN}$ ,<sup>9d</sup>  $\text{ClXeCN}$ ,<sup>29a</sup>  $\text{BrXeCN}$ ,<sup>29a</sup>  $\text{HXeCCH}$ ,<sup>29b</sup>  $\text{HXeCCXeH}$ ,<sup>10d</sup>  $\text{HXeCCF}$ ,<sup>29c</sup>  $\text{HXeC}_3\text{N}$ <sup>29d</sup> and  $\text{HXeC}_4\text{H}$ <sup>9j</sup> were reported. Theoretical studies have also immensely contributed to the discovery of different xenon-carbon compounds.<sup>30</sup> Efforts towards syntheses of compounds with Xe-Si and Xe-Ge bonds are currently being explored. The gaseous trifluorosilylxenon,  $\text{F}_3\text{Si-Xe}^+$  was detected by spectroscopic techniques, and, also examined by computations.<sup>31,32</sup> We have recently assessed the stability of  $\text{NgSiX}_3^+$  ( $\text{X} = \text{H}, \text{F-Br}$ ) clusters.<sup>15h</sup> The inserted Xe compound on  $\text{SiF}_2$  resulting in the formulation of  $\text{FXeSiF}$ <sup>33</sup> was also reported. Recently, the gaseous trifluorogermylxenon cation,  $\text{F}_3\text{Ge-Xe}^+$  was observed by means of mass spectroscopic techniques.<sup>34</sup> Grandinetti and co-workers<sup>35</sup> explored the stability of neutral  $\text{FXeGeF}_n$  ( $n = 1, 3$ ) compounds with xenon-germanium bonds. They showed that such molecules are thermochemically stable with respect to all possible dissociation channels except the dissociation into  $\text{Xe} + \text{GeF}_{n+1}$ ; however, they are kinetically stable with respect to that dissociation. Yockel et al.<sup>36</sup> theoretically predicted the stability of  $\text{FKrGeF}_3$ , the only known neutral compound with Kr-Ge bond. Chemistry related to the

Ng-compounds having bonds between Ng and heavier congeners than Ge is still unexplored.

The present study is an effort to bridge that gap. Here, we have presented for the first time the neutral compounds, FNgEF<sub>3</sub> and FNgEF (Ng = Kr, Xe, Rn; E = Sn, Pb) having Ng-Sn and Ng-Pb bonds. Their thermochemical and kinetic stabilities are assessed by computing the dissociation energy, enthalpy change, free energy change and activation barrier of different probable dissociation channels. FNgSnF<sub>3</sub> (Ng = Xe, Rn) and FNgEF (Ng = Kr, Xe, Rn) are found to be thermochemically stable with respect to all probable dissociation channels except a two-body dissociation channel producing Ng and EF<sub>4</sub> or EF<sub>2</sub>. FNgPbF<sub>3</sub> compounds are found to be thermochemically unstable with respect to two two-body dissociation channels. However, they are kinetically protected with respect to these dissociations. The bonding situation is analyzed by natural bond order, electron density and energy decomposition analyses.

### Computational Details

The geometry optimizations for all the studied systems are performed at the MP2<sup>37</sup>/def2-TZVPPD<sup>38</sup> level by using the Gaussian 09 program package.<sup>39</sup> A quasi-relativistic pseudopotential is used for core electrons of Sn, Pb, Xe, and Rn atoms.<sup>40</sup> The characterization of the stationary state as of minimum energy or transition state (TS) is done by computing harmonic vibrational frequencies. We have also computed intrinsic reaction coordinates (IRC) to ensure that the transition states are connected with the desired minima along the minimum energy path (see Figure S1 in the supporting information). Taking the FNgEF set (E = Sn, Pb), optimizations and frequency calculations are also carried out at the CCSD(T)<sup>41</sup>/def2-TZVP<sup>39</sup> level to ensure that these minima are not an artifact of the MP2 level. The structural parameters obtained from the CCSD(T)/def2-TZVP computations are provided in Table S1 (supporting information) and here we continue with the results obtained at the MP2/def2-TZVPPD level. The natural bond order (NBO) analysis is performed as implemented within Gaussian 09 program.<sup>39</sup> The atoms-in-molecules (AIM)<sup>42</sup> analysis is carried out by using Multiwfn software<sup>43</sup> at the MP2/def2-TZVPPD/WTBS<sup>44</sup> level taking the optimized geometries at the MP2/def2-TZVPPD level. All electron WTBS<sup>44</sup> basis set is used for Sn, Pb, Xe, and

Rn. The electron density ( $\rho(r_c)$ ), the Laplacian of the electron density ( $\nabla^2\rho(r_c)$ ), the total electron energy density ( $H(r_c)$ ), the local kinetic energy density ( $G(r_c)$ ) and the local potential energy density ( $V(r_c)$ ) at the bond critical points (BCPs) are also computed. We have further considered the classifications as was done by Boggs and co-workers.<sup>45</sup> They classified the covalent bonds into four types:

Type A.  $\nabla^2\rho(r_c) < 0$ , and  $\rho(r_c)$  is large ( $\geq 0.1$  au)

Type B.  $H(r_c) < 0$ , and  $\rho(r_c)$  is large ( $\geq 0.1$  au)

Type C.  $H(r_c) < 0$ , and  $G(r_c)/\rho(r_c) < 1$

Type D.  $|H(r_c)|$  is small ( $< 0.005$  au) and  $G(r_c)/\rho(r_c) < 1$

The same authors<sup>45</sup> also proposed two new categories viz.,  $W^c$  (weak interaction having some degree of covalent character) and  $W^n$  (weak interaction having noncovalent character) depending on the bond lengths.

The energy decomposition analysis<sup>46</sup> (EDA) is carried out at the revPBE-D3<sup>47</sup>/TZ2P<sup>48</sup>//MP2/def2-TZVPPD level using ADF(2013.01) program package.<sup>49</sup> Scalar relativistic effects are included for the heavier atoms using the zeroth-order regular approximation (ZORA).<sup>50</sup>

### Structure and stability

The structures of the minimum energy states and transition states of FNgEF<sub>3</sub> and FNgEF (E = Sn, Pb; Ng = Kr-Rn) compounds are pictorially depicted in Fig. 1. All the FNgEF<sub>3</sub> compounds correspond to  $C_{3v}$  point group with  $^1A_1$  electronic state. However, their geometries change to have a  $C_s$  point group while they pass through transition state structure corresponding to the dissociation of FNgEF<sub>3</sub> into Ng and EF<sub>4</sub> (**TS-1** in Fig. 1). On the other hand, all FNgEF compounds have planar geometries with  $C_s$  point group and  $^1A'$  electronic states which adopt non-planar geometries having  $C_1$  point group in the transition states associated with the dissociation of FNgEF into Ng and EF<sub>2</sub> (**TS-2** in Fig. 1). The transition states obtained for the dissociation of FNgPbF<sub>3</sub> into NgF<sub>2</sub> and PbF<sub>2</sub> also correspond to  $C_1$  point group (**TS-3** in Fig. 1). The possibility of the existence of higher spin states is also verified but they are found to be higher energy structures.

The different geometrical parameters of these FNgEF<sub>3</sub> and FNgEF compounds along with their transition state structures are provided in Tables S2 and S3 (Supporting

Information). The F-Ng-E moieties in FNgEF<sub>3</sub> compounds are linear. The Ng-E-F angle gradually increases from Kr to Rn. It shows that the bending of F-E-F moieties in EF<sub>3</sub> away from the bound Ng direction becomes gradually larger in heavier Ng bound analogues, being the largest in Rn case. In the energy minimum structures of FNgEF compounds, the F-Ng, Ng-E and Sn-F bond distances are somewhat larger than those in FNgEF<sub>3</sub> revealing their less compactness. Unlike FNgEF<sub>3</sub>, the F-Ng-E moieties in FNgEF are not perfectly linear, rather somewhat (*ca.* 0.1°-3.6°) bent from the absolutely linear arrangement. In **TS-1** and **TS-2**, the F atom is bonded to Ng in a tilted fashion with the mode of imaginary frequency as the bending of F-Ng-Sn having F-Ng-E angle of 95.0°-130.6°. In **TS-3**, one F atom in PbF<sub>3</sub> is found to be in a bridging position in between Pb and Ng. The mode of the imaginary frequency is associated with the shifting of this bridging F center towards Ng atom and other F atom attached with Ng atom moves in such a fashion that it gives NgF<sub>2</sub> a linear structure. The Pb-F (bridged) bond length is larger by about 0.1 Å than the other two Pb-F bonds. The Pb-Ng bonds are also found to be larger by 0.19 Å in Xe and 0.16 Å in Rn analogues than those in the corresponding minimum energy structures (see Table S3 in supporting information).

Other detailed geometrical changes in moving from minimum energy structures to the respective transition states or from Kr compounds to their heavier analogues are provided in the supporting information. It may be noted that the Ng-E bond lengths in FNgEF are somewhat larger than those in FNgEF<sub>3</sub>. The shorter Ng-E distances in FNgEF<sub>3</sub> may be related to the fact that the Ng atoms in FNgEF<sub>3</sub> bear larger positive charge (ranging +0.49 to +0.94 *e*<sup>-</sup>) than those in FNgEF (ranging +0.20 to +0.44 *e*<sup>-</sup>). Ng atoms generally do not take part in chemical bonding due to their fulfilled valence shell configuration. Therefore, the Ng atoms having larger positive charge would be more effective candidates in forming chemical bond than that having less positive charge. An anomalous result is found in FKrPbF, where the Kr-Pb bond length is about 0.04 Å shorter than that in FKrPbF<sub>3</sub>.

The IR frequencies along with the IR intensities for different vibrational modes of FNgEF<sub>3</sub> and FNgEF compounds are tabulated in Tables S4 and S5 and discussed in the supporting information.

In order to understand the stability of presently investigated compounds, ZPE corrected dissociation energy ( $D_0$ ), dissociation enthalpy ( $\Delta H$ ) and free energy change ( $\Delta G$ ) for different dissociation channels of  $\text{FNgEF}_3$  and  $\text{FNgEF}$  compounds computed at the MP2/def2-TZVPPD level are displayed in Tables 1 and 2. Here,  $\Delta H$  and  $\Delta G$  values are calculated at 298.15 K. The dissociation pathways are illustrated by Eqs. 1 - 4 (here,  $n = 1, 3$ ):



The three-body (3-B) dissociations for all  $\text{FNgEF}_3$  and  $\text{FNgEF}$  compounds are shown to be endothermic; however, the dissociation processes of  $\text{FNgEF}$  are more endothermic than those of  $\text{FNgEF}_3$ . For  $\text{FKrPbF}_3$ , the  $D_0$  value is negative (-0.2 kcal/mol) and 3-B dissociation is only slightly endothermic in nature ( $\Delta H = 0.3$  kcal/mol). In case of  $\text{FKrSnF}_3$ , the dissociation energy ( $D_0 = 7.6$  kcal/mol) and endothermicity ( $\Delta H = 8.2$  kcal/mol) are also quite low. In such dissociation process, since entropy change ( $\Delta S$  is positive) is a favorable term, we have also computed free energy change ( $\Delta G$ ). The 3-B dissociations of  $\text{FKrEF}_3$  compounds are spontaneous at room temperature as indicated by negative values (-7.8 and -14.8 kcal/mol for  $\text{FKrSnF}_3$  and  $\text{FKrPbF}_3$ , respectively) of  $\Delta G$ . Except  $\text{FKrEF}_3$ , in all other cases the unfavorable  $\Delta H$  values for these 3-B dissociations are so large that favorable  $\Delta S$  term cannot overshadow them. In both  $\text{FNgEF}_3$  and  $\text{FNgEF}$  cases, the stability with respect to the 3-B dissociation gradually improves along Kr to Rn. This corroborates well with the WBI values of Ng-Sn bonds, which depict more covalent character in moving from Kr to Rn (*vide infra*). Note that despite higher WBIs and compactness in  $\text{FNgEF}_3$  than those in  $\text{FNgEF}$ , the corresponding  $D_0$  values for the 3-B channels are smaller in the former case than that in the latter. The difference in the stability of dissociated  $\text{EF}_3$  and  $\text{EF}$  products and the charge on the respective atoms of the bound systems are presumably the reasons behind this.

The two-body (2-B) dissociations (Eq. 2) of  $\text{FNgSnF}_3$  and  $\text{FNgSnF}$  producing  $\text{NgF}_2$  and  $\text{SnF}_2$  or  $\text{Sn}$  are also endergonic in nature, which are more unfavorable in latter



cases than those in the former. However, unlike Ng-Sn complexes, this 2-B dissociation of  $\text{FNgPbF}_3$  generating  $\text{NgF}_2$  and  $\text{PbF}_2$  are exergonic in nature at room temperature. The activation barriers ( $\Delta E^\ddagger$ ) for this dissociation are found to be 13.8 kcal/mol for Xe and 10.1 kcal/mol for Rn complexes. On the other hand, the dissociations of  $\text{FNgPbF}$  resulting in  $\text{NgF}_2$  and Pb are highly endergonic in nature.

The  $D_0$  values corresponding to the ionic dissociations following Eq. 3 are significantly higher in comparison to that in Eq. 2 in  $\text{FNgSnF}_3$  whereas the same is smaller in  $\text{FNgEF}$  cases. Note that the ionic dissociations for  $\text{FNgEF}_3$  are more endergonic in nature than those in  $\text{FNgEF}$ . The 2-B dissociations of  $\text{FNgEF}_3$  and  $\text{FNgEF}$  as Ng and  $\text{EF}_{(n+1)}$  (Eq. 4) are highly exergonic in nature. The dissociations of  $\text{FKrSnF}_3$  and  $\text{FKrSnF}$  producing Kr and  $\text{SnF}_4$  or  $\text{SnF}_2$  are almost equally exergonic whereas for Xe and Rn analogues of  $\text{FNgSnF}_3$  and  $\text{FNgPbF}_3$  compounds, this 2-B dissociation is slightly less spontaneous in nature than those in  $\text{FNgEF}$ . However, the  $\Delta E^\ddagger$  values computed for these dissociation processes are positive, being reasonably high for  $\text{FNgFF}_3$  but quite low for  $\text{FNgEF}$ . The  $\Delta E^\ddagger$  values are 23.9, 32.7 and 36.8 kcal/mol for Kr, Xe and Rn analogues of  $\text{FNgSnF}_3$ , respectively, whereas, the same are 2.9, 6.9 and 8.7 kcal/mol for Kr, Xe and Rn analogues of  $\text{FNgSnF}$ , respectively. On the other hand, for  $\text{FNgPbF}_3$  the  $\Delta E^\ddagger$  values are quite larger than those in  $\text{FNgSnF}_3$  being 40.5 for Kr, 46.6 for Xe and 49.9 kcal/mol for Rn analogues whereas for  $\text{FNgPbF}$ , the  $\Delta E^\ddagger$  values are slightly smaller than those in  $\text{FNgSnF}$  being 2.2 for Kr, 6.0 for Xe and 7.8 kcal/mol for Rn analogues. Therefore, for a particular type of compounds, the barrier gradually increases in moving from Kr to Rn analogues.

In all cases here,  $\Delta E^\ddagger$  values are found to be larger with the increased WBI values of Ng-E bonds. Now, let us compare the barrier in the present cases with those found by Hu and co-workers<sup>51</sup> in  $\text{XNgY}$  type of systems. They argued that 2-B dissociation channel for a system as per Eqs. 2 and 4 must have a minimum barrier of 6, 13 and 21 kcal/mol to have a half-life of 100 s in the gas phase at 100, 200 and 300 K, respectively. Therefore, all  $\text{FNgSnF}_3$  compounds should be metastable at 300 K or even at higher temperature whereas  $\text{FXeEF}$  and  $\text{FRnEF}$  might be detectable at least at 100 K. Due to very low barrier,  $\text{FKrEF}$  is very unlikely to be detected. Although the barrier for the dissociations of  $\text{FNgPbF}_3$  following Eq. 4 is large enough to exist at 300K or even at

higher temperature but the barrier corresponding to the dissociation producing  $\text{NgF}_2$  and  $\text{PbF}_2$  (Eq. 2) implies that  $\text{FXePbF}_3$  could be metastable up to 200 K whereas for  $\text{FRnPbF}_3$  lower temperature is needed. The instability of  $\text{FKrEF}_3$  towards the 3-B dissociation channel also rules out the possibility of its detection.

### Nature of bonding

To get an idea about the bonding situation we have computed atomic charges derived from the natural population analysis (NPA) and Wiberg bond indices (WBIs) for each bond of  $\text{FNgEF}_3$  and  $\text{FNgEF}$  compounds (see Table 3). According to NPA charge, in both  $\text{FNgEF}_3$  and  $\text{FNgEF}$  all F atoms bear negative charges and Ng and E possess positive charges. Ng bears less positive charge in comparison to E atom in all cases. Positive charge on Ng increases on moving from Kr to Rn systems, whereas the positive charge on E decreases along the same. F atom attached to Ng contains more negative charge in comparison to the fluorine atom attached to E except in the cases of  $\text{FKrPbF}_3$  and  $\text{FXePbF}_3$ , in which the reverse is true. Further, the charge on F bonded to Ng atom is less negative for  $\text{FNgEF}_3$  systems (range  $-0.69$  to  $-0.83 e^-$ ) than that in  $\text{FNgEF}$  systems (range  $-0.92$  to  $-0.94 e^-$ ). The positive charges on Ng and E centers are comparatively less in  $\text{FNgEF}$  compounds than those in  $\text{FNgEF}_3$ . Following the charge distribution, these systems could be best represented as  $\text{F}-(\text{NgEF}_3)^+$  and  $\text{F}-(\text{NgEF})^+$ . Consequently, the F-Ng bond is essentially an ionic bond. The very low WBI values for F-Ng bonds also describe their ionic character. The F-Ng bonds in  $\text{FNgEF}$  are even more ionic in nature as indicated by lower WBIs and higher negative charge on F than those in  $\text{FNgEF}_3$ .

In contrast, the Ng-E bonds appear to be covalent in nature. In  $\text{FNgEF}_3$ , the WBIs of Ng-E bonds are within the range of 0.60 to 0.82 whereas those in  $\text{FNgEF}$  are somewhat smaller than the former cases ranging within 0.38-0.70. Therefore, the degree of covalent character in Ng-E bonds gradually increases in moving from Kr to Rn analogues as indicated by the increased WBI values along the same. Note that lower WBIs for Ng-E bonds in  $\text{FNgEF}$  than  $\text{FNgEF}_3$  corroborate well with the fact that the Ng-E bond distances in the latter are shorter than those in the former.

Now, electron density analysis<sup>42</sup> is performed to get more insight into the nature of bonding. Table 4 presents different topological descriptors at the BCPs of F-Ng and

Ng-E bonds of FNgEF<sub>3</sub> and FNgEF compounds along with the typical covalent bond distance computed for F-Ng and Ng-E bonds following the studies of Cordero et al.<sup>52</sup> and Pyykkö.<sup>53</sup> In general, negative (electron density concentration) and positive (electron density depletion) values of  $\nabla^2\rho(r_c)$  at the BCPs are indicators of covalent and noncovalent bonding, respectively. However, in many cases including the systems containing 3d and heavier atoms it fails to explain a covalent bond (for examples see ref. 54 and pp. 312-314 of ref. 42).

Some other criteria to interpret a covalent bond are also reported in the literature. Such as, if  $\nabla^2\rho(r_c) > 0$  and  $H(r_c) < 0$  or  $G(r_c)/\rho(r_c) < 1$ , then the bond might be regarded as a partial covalent bond.<sup>55,56</sup> Moreover, in order to interpret the nature of bonding, we have also included the classifications suggested by Boggs et al.<sup>45</sup> as described in computational details section. Since in all cases  $\nabla^2\rho(r_c)$  is positive, therefore it rules out the possibility of type A. The contour plots of  $\nabla^2\rho(r_c)$  for FNgEF<sub>3</sub> and FNgEF are provided in Figs. 2 and S2 (in supporting information), respectively. No charge concentration is found in between two atoms. Only the shapes of valence orbitals get slightly deformed. Note that  $H(r_c)$  values at the BCPs of both F-Ng and Ng-E bonds are negative, even it is more negative in F-Ng bonds than those in Ng-E bonds except FKrEF compounds. On the other hand,  $G(r_c)/\rho(r_c)$  values are very small (<0.8) in Ng-E bonds whereas it exceeds the limiting value of 1 in the cases of F-Ng bonds except for the F-Ng bonds in FKrEF<sub>3</sub>. Therefore, if we follow Boggs' classification,<sup>45</sup> we need to categorize the F-Ng bonds in FKrEF<sub>3</sub> as of types B and C both whereas the rest of the F-Ng bonds as of W<sup>c</sup> type. However, we have already seen that it would be the best to consider these F-Ng bonds as of ionic type (*vide supra*). It indicates that such classification does not always lead to proper conclusion. All Ng-E bonds fall in the category of C with the criteria of  $H(r_c) < 0$ , and  $G(r_c)/\rho(r_c) < 1$ .

It may be noted that in FNgSnF<sub>3</sub>, the Kr-Sn equilibrium bond distance ( $r_e$ ) is only 0.07<sup>52</sup>/0.05<sup>53</sup> Å larger than that of corresponding covalent bond distance ( $r_{cov}$ ) whereas for Xe-Sn and Rn-Sn,  $r_e$  values fall perfectly in the range of their reported  $r_{cov}$  distances. Therefore, considering their high WBI values, we may treat them as covalent bonds. In FNgSnF compounds,  $r_e$  values of Ng-Sn bonds are 0.13<sup>52</sup>/0.11<sup>53</sup> Å for Kr, 0.06<sup>52</sup>/0.14<sup>53</sup> Å for Xe and 0.04<sup>52</sup>/0.11<sup>53</sup> Å for Rn larger than the corresponding  $r_{cov}$  values. Therefore,

here also from their WBI values, Xe/Rn-Sn bonds might be called as covalent bonds whereas Kr-Sn might be the border line case between the partial and perfect covalent bonds. In FNgPbF<sub>3</sub>, the Xe-Pb and Rn-Pb bond distances are almost equal to their  $r_{\text{cov}}$  distances whereas in FNgPbF compounds,  $r_e$  values of Ng-Pb bonds are 0.18<sup>52</sup>/0.19<sup>53</sup> Å for Kr, 0.06<sup>52</sup>/0.17<sup>53</sup> Å for Xe and 0.03<sup>52</sup>/0.13<sup>53</sup> Å for Rn larger than the corresponding  $r_{\text{cov}}$  values. Therefore, Xe-Pb and Rn-Pb bonds could also be called as covalent bonds.

It may also be noted that the descriptor,  $G(r_c)/\rho(r_c)$  represents the bonding situation in the present systems most appropriately. It is around 1 for F-Ng bonds and it is much smaller than 1 for Ng-E bonds. It even gradually decreases for Ng-E bonds along Kr to Rn showing larger covalent character along the same. Further, this value for Ng-E bond is somewhat smaller in FNgEF<sub>3</sub> than those in FNgEF implying larger covalency in the former than that in the latter. Therefore, it perfectly tallies with the WBI results.  $\nabla^2\rho(r_c)$  does not seem to describe these systems properly.

EDA<sup>46</sup> is also performed to get an idea about the contribution from Pauli repulsion ( $\Delta E_{\text{pauli}}$ ), electrostatic ( $E_{\text{elstat}}$ ), orbital ( $\Delta E_{\text{orb}}$ ) and dispersion ( $\Delta E_{\text{disp}}$ ) energy terms towards the total interaction energy ( $\Delta E_{\text{int}}$ ) (see Tables 5 and 6). We have followed the NPA charges obtained on each center to impose the overall charge on a fragment. Since both FNgEF<sub>3</sub> and FNgEF could be best represented as  $\text{F}^-(\text{NgEF}_3)^+$  and  $\text{F}^-(\text{NgEF})^+$ , to explore the nature of bonding in F-Ng bonds we have partitioned FNgEF<sub>3</sub> and FNgEF into  $\text{F}^-$  and  $[\text{NgEF}_3]^+$  or  $[\text{NgEF}]^+$ . In FNgEF<sub>3</sub> compounds, since the total charges on fragments [FNg] and [EF<sub>3</sub>] are well below  $|0.5| e^-$ , we have considered them as neutral (radical). However, in FNgEF compounds except FRnSnF, the charges on [FNg] and [EF] fragments are larger than  $|0.5| e^-$ . Therefore, for these cases we have performed EDA by considering both radical and charged fragments. The preparation energies of these fragments, interaction energies and dissociation energies computed at the MP2/def2-TZVPPD level are provided in Tables S6 and S7 (supporting information). As expected from the ionic character, in F-Ng bonds the contribution from  $\Delta E_{\text{elstat}}$  is dominant ranging from 60 to 70% towards the total attraction. It may be noted that the contribution from  $\Delta E_{\text{orb}}$  is also quite large (*ca.* 30-40%) in F-Ng bonds.  $\Delta E_{\text{disp}}$  term is not at all important since it contributes the least. In the cases of Ng-E bonds in FNgEF<sub>3</sub>,  $\Delta E_{\text{orb}}$  is the largest contributor (*ca.* 72-82%) towards the total attraction. Such large

contribution from  $\Delta E_{\text{orb}}$  indicates the nature of Ng-E bonds in FNgEF<sub>3</sub> as of covalent type. For these Ng-E bonds,  $\Delta E_{\text{elstat}}$  contributes around 17-27% towards the total attraction. In Ng-E bonds of FNgEF, use of charged fragments leads to  $\Delta E_{\text{elstat}}$  (*ca.* 61-65%) term dominant over  $\Delta E_{\text{orb}}$  (*ca.* 35-38%) whereas the partition into radical fragments yields  $\Delta E_{\text{orb}}$  as the major contributing term (*ca.* 75-79%) towards the total attraction. Therefore, the choice of nature of fragments alters the dominating term in the bonding. It may be noted that in FXeSnF and FRnSnF, the charges on each individual fragment are  $|0.55| e^-$  and  $|0.48| e^-$ , respectively, whereas in FXePbF and FRnPbF, the charges on each fragment are  $|0.59| e^-$  and  $|0.52| e^-$ , respectively. Therefore, neither of these two partitioning schemes would represent the actual situation.

### Comparison with FXeGeF<sub>3</sub> and FXeGeF

To compare our present FXeEF<sub>3</sub> and FXeEF cases with FXeGeF<sub>3</sub> and FXeGeF reported by Grandinetti et al.<sup>35</sup>, we have reoptimized the structures at the same MP2/def2-TZVPPD level. The different geometrical parameters along with a comparative discussion are provided in the supporting information (see Table S8). Here, we have only discussed about their thermochemical and kinetic stabilities and nature of bonding.

The ZPE corrected dissociation energy, dissociation enthalpy and free energy changes for different dissociation channels of FXeGeF<sub>3</sub> and FXeGeF are given in Table S9 (supporting information). It may be noted that the 3-B (Eq. 1) and 2-B dissociation channels (Eq. 2) are more endothermic and thermochemically unfavorable for FXeGeF<sub>3</sub> compounds than those of Sn and Pb-analogues whereas the ionic 2-B dissociation channels (Eq. 3) are almost equally unfavorable with Sn-analogue. The dissociation of FXeGeF<sub>3</sub> into Xe and GeF<sub>4</sub> is more feasible by 14.5 and 42.3 kcal/mol than those of FXeSnF<sub>3</sub> and FXePbF<sub>3</sub>, respectively. The corresponding barrier for the dissociation process of FXeGeF<sub>3</sub> is 1.5 kcal/mol smaller than that in FXeSnF<sub>3</sub> whereas it is 15.4 kcal/mol smaller than that in FXePbF<sub>3</sub>. In FXeGeF, the 3-B dissociation is only slightly less unfavorable and other two 2-B dissociations (Eqs. 2 and 3) are more unfavorable than those in FXeSnF and FXePbF. On the other hand, although the dissociation of FXeGeF producing Xe and GeF<sub>2</sub> is more spontaneous than those of FXeSnF and

FXePbF, the barrier is 1.8 and 2.7 kcal/mol larger in the former than those in the latter cases, respectively. Therefore, FXeGeF is more kinetically protected with respect to this dissociation channel than FXeSnF and FXePbF.

NPA reveals that the F-Xe bond in FXeGeF<sub>3</sub> is more polarized than those in FXeSnF<sub>3</sub> and FXePbF<sub>3</sub> but the same in FXeGeF is less polarized compared to FXeSnF and FXePbF (see Table S10 in supporting information). In FNgEF<sub>3</sub>, the positive charge on Ge center is slightly less than that on Sn center but larger than that on Pb center. The WBI value of Xe-Ge bond in FXeGeF<sub>3</sub> (0.720) is only slightly smaller than those in FXeSnF<sub>3</sub> and FXePbF<sub>3</sub> whereas in FXeGeF the WBI value of Xe-Ge bond is larger than those in the other two compounds.

Different electron density descriptors at the BCPs of F-Xe and Xe-Ge bonds show that they can be categorized as types W<sup>c</sup> and C, respectively, similar to those of Xe-Sn and Xe-Pb compounds (see Table S11 in supporting information). However, unlike Xe-Sn and Xe-Pb compounds,  $\nabla^2\rho(r_c)$  is negative for Xe-Ge bonds representing the nature of these bonds perfectly. The values of  $H(r_c)$  and  $G(r_c)/\rho(r_c)$  in both cases are quite comparable,  $H(r_c)$  being slightly more negative and  $G(r_c)/\rho(r_c)$  being slightly less positive in Xe-Ge bonds than those in Xe-Sn and Xe-Pb bonds.

## Conclusion

FNgEF<sub>3</sub> and FNgEF (E = Sn, Pb; Ng=Kr, Xe, Rn) compounds might be considered to be the first reported cases of systems having Ng-Sn and Ng-Pb bonds. FKrEF<sub>3</sub> compounds are not viable since they are predicted to dissociate spontaneously along a 3-B dissociation channel producing F, Kr and EF<sub>3</sub>. The other Ng-Sn compounds are thermochemically stable with respect to all possible dissociation channels except a 2-B dissociation channel, which results in the formation of Ng and SnF<sub>4</sub> or SnF<sub>2</sub>. However, they are kinetically stable with respect to this dissociation channel. The activation barrier is larger in FNgSnF<sub>3</sub> (23.9-36.8 kcal/mol) than that in FNgSnF (2.9-8.7 kcal/mol) showing higher kinetic stability in the former cases than the latter. The dissociation of FNgPbF<sub>3</sub> (Ng = Xe, Rn) compounds is found to be exergonic along two 2-B dissociation channels. The activation barrier for the dissociation of FNgPbF<sub>3</sub> into NgF<sub>2</sub> and PbF<sub>2</sub> is 13.8 kcal/mol for Xe and 10.1 kcal/mol for Rn whereas the same for the dissociation into

Ng and PbF<sub>4</sub> is 46.6 kcal/mol for Xe and 49.9 kcal/mol for Rn. On the other hand, FNgPbF compounds are found to be thermochemically stable with respect to all possible dissociation channels except the dissociation into Ng and PbF<sub>2</sub>. The corresponding activation barrier is quite low ranging within 2.2-7.8 kcal/mol. For a particular series, the kinetic stability gradually increases along Kr to Rn analogues. Following an argument of Hu et al.,<sup>51</sup> all FNgSnF<sub>3</sub> compounds are predicted to be stable at 300 K or even higher whereas FRnPbF<sub>3</sub>, FXeEF and FRnEF might be metastable at around 100 K. FXePbF<sub>3</sub> might be detected at 200 K. The very low barrier suggests the instability of FKrEF to be in such bound forms at even very low temperature. NPA suggests that these structures could be best represented as F<sup>-</sup>(NgEF<sub>3</sub>)<sup>+</sup> and F<sup>-</sup>(NgEF)<sup>+</sup>. WBI values of Ng-E bonds are quite high ranging from 0.60 to 0.82 in FNgEF<sub>3</sub> whereas it is slightly lower in FNgEF ranging in between 0.38 and 0.70 with a gradual increment along Kr to Rn. From EDA, WBI and the bond lengths, the Xe/Rn-E bonds in FNgEF<sub>3</sub> and FNgEF might be termed as covalent bonds whereas Kr-E bond in FNgEF is a borderline case between partial and perfect covalent bonds. EDA shows that in F-Ng bonds, mainly  $\Delta E_{\text{elstat}}$  contributes towards the total attraction implying their ionic character whereas in the Ng-E bonds of FNgEF<sub>3</sub> the contribution from  $\Delta E_{\text{orb}}$  is the maximum showing their covalent character. In the Ng-E bonds of FNgEF, the partition into the charged fragments ([FNg]<sup>-</sup> + [EF]<sup>+</sup>) gives  $\Delta E_{\text{elstat}}$  as the major contributor but the consideration of the neutral fragments provides  $\Delta E_{\text{orb}}$  as the most dominant term.

### Acknowledgements

PKC would like to thank DST, New Delhi for the J. C. Bose National Fellowship. SP thanks CSIR, New Delhi for his fellowship. AG thanks UGC for Major Research Grant (2013-2016) for the current project (F.No. 42-256/2013 (SR)). Conacyt (Grant INFRA-2013-01-204586) and Moshinsky Foundation supported the work in Mérida. DM thanks Conacyt for his Ph.D fellowship.

### References

1. A. von Antropoff, K. Weil and H. Frauenhof, *Naturwissenschaften* 1932, **20**, 688.
2. W. Kossel, *Annalen der Physik* 1916, **49**, 229.

3. L. Pauling, *J. Am. Chem. Soc.* 1932, **54**, 3570.
4. D. M. Yost and A. L. Kaye, *J. Am. Chem. Soc.* 1933, **55**, 3890.
5. N. Bartlett, *Proc. Chem. Soc.* 1962, 218.
6. H. H. Claassen, H. Selig and J. G. Malm, *J. Am. Chem. Soc.* 1962, **84**, 3593.
7. J. Slivnik, B. Brcic, B. Volavsek, A. Smalc, B. Frlec, R. Zemljic, A. Anzur and Z. Vekšli, *Croat. Chem. Acta* 1962, 34.
8. R. Hoppe, W. Dähne, H. Mattauch and K. Rödder, *Angew. Chem. Int. Ed.* 1962, **1**, 599.
9. a) M. Pettersson, J. Lundell and M. Räsänen, *J. Chem. Phys.*, 1995, **103**, 205; b) M. Pettersson, J. Nieminen, L. Khriachtchev and M. Räsänen, *J. Chem. Phys.*, 1997, **107**, 8423; c) M. Pettersson, J. Lundell, L. Isamieni and M. Räsänen, *J. Am. Chem. Soc.*, 1998, **120**, 7979; d) M. Pettersson, J. Lundell, L. Khriachtchev and M. Räsänen, *J. Chem. Phys.*, 1998, **109**, 618; e) M. Pettersson, L. Khriachtchev, J. Lundell and M. Räsänen, *J. Am. Chem. Soc.*, 1999, **121**, 11904; f) L. Khriachtchev, M. Pettersson, N. Runeberg, J. Lundell and M. Räsänen, *Nature*, 2000, **406**, 874; g) L. Khriachtchev, M. Pettersson, A. Lignell and M. Räsänen, *J. Am. Chem. Soc.*, 2001, **123**, 8610; h) L. Khriachtchev, M. Pettersson, J. Lundell, H. Tanskanen, T. Kiviniemi, N. Runeberg and M. Räsänen, *J. Am. Chem. Soc.*, 2003, **125**, 1454; i) L. Khriachtchev, H. Tanskanen, A. Cohen, R. B. Gerber, J. Lundell, M. Pettersson, H. Kiljunen and M. Räsänen, *J. Am. Chem. Soc.*, 2003, **125**, 6876; j) H. Tanskanen, L. Khriachtchev, J. Lundell, H. Kiljunen and M. Räsänen, *J. Am. Chem. Soc.*, 2003, **125**, 16361.
10. a) V. I. Feldman and F. F. Sukhov, *Chem. Phys. Lett.*, 1996, **225**, 425; b) V. I. Feldman, F. F. Sukhov and A. Y. Orlov, *Chem. Phys. Lett.*, 1997, **280**, 507; c) L. Khriachtchev, H. Tanskanen, M. Pettersson, M. Rasanen, J. Ahokas, H. Kunttu and V. Feldman, *J. Chem. Phys.* 2002, **116**, 5649; d) V. I. Feldman, F. F. Sukhov, A. Yu. Orlov and I. V. Tyulпина, *J. Am. Chem. Soc.*, 2003, **125**, 4698; e) V. I. Feldman, A. V. Kobzarenko, I. A. Baranova, A. V. Danchenko, F. F. Sukhov, E. Tsivion and R. B. Gerber, *J. Chem. Phys.*, 2009, **131**, 151101; f) S. V. Ryazantsev, A. V. Kobzarenko and V. I. Feldman, *J. Chem. Phys.*, 2013, **139**, 124315.
11. a) C. A. Thompson and L. Andrews, *J. Am. Chem. Soc.*, 1994, **116**, 423; b) C. A. Thompson and L. Andrews, *J. Chem. Phys.*, 1994, **100**, 8689; c) X. Wang, L. Andrews, K. Willmann, F. Brosi and S. Riedel, *Angew. Chem., Int. Ed.*, 2012, **51**, 10628; d) J. Li, B. E. Bursten, B. Liang, and L. Andrews, *Science*, 2002, **295**, 2242. e) B. Liang, L. Andrews, J. Li, and B. E. Bursten, *J. Am. Chem. Soc.* 2002, **124**, 9016; f) X. Wang, L. Andrews, J. Li, and B. E. Bursten, *Angew. Chem. Int. Ed.* 2004, **43**, 2554.
12. a) C. J. Evans and M. C. L. Gerry, *J. Chem. Phys.*, 2000, **112**, 1321; b) C. J. Evans and M. C. L. Gerry, *J. Chem. Phys.*, 2000, **112**, 9363; c) C. J. Evans, D. S. Rubinoff and M. C. L. Gerry, *Phys. Chem. Chem. Phys.*, 2000, **2**, 3943; d) C. J. Evans, A. Lesarri and M. C. L. Gerry, *J. Am. Chem. Soc.*, 2000, **122**, 6100; e) L. M. Reynard, C. J. Evans and M. C. L. Gerry, *J. Mol. Spectrosc.*, 2001, **206**, 33; f) N. R. Walker, L. M. Reynard and M. C. L. Gerry, *J. Mol. Struct.*, 2002, **612**, 109; g) J. M. Michaud, S. A. Cooke and M. C. L. Gerry, *Inorg. Chem.*, 2004, **43**, 3871; h) J. M. Thomas, N. R. Walker, S. A. Cooke and M. C. L. Gerry, *J. Am. Chem. Soc.*, 2004, **126**, 1235; i) S. A. Cooke and M. C. L. Gerry, *Phys. Chem. Chem. Phys.*, 2004, **6**, 3248; j) S. A. Cooke and M. C. L. Gerry, *J. Am. Chem. Soc.*, 2004, **126**, 17000; k) J. M. Michaud and M. C. L. Gerry, *J. Am. Chem. Soc.*, 2006, **128**, 7613.



13. a) A. A. Emara and G. J. Schrobilgen, *Inorg. Chem.*, 1992, **31**, 1323; b) G. A. Schumacher and G. J. Schrobilgen, *Inorg. Chem.*, 1983, **22**, 2178; c) G. L. Smith, H. P. Mercier and G. J. Schrobilgen, *Inorg. Chem.*, 2007, **46**, 1369; d) G. J. Schrobilgen, *J. Chem. Soc. Chem. Comm.*, 1988, **13**, 863. e) M. Hughes, D. S. Brock, H. P. A. Mercier and G. J. Schrobilgen, *J. Fluorine Chem.*, 2011, **132**, 660; f) G. L. Smith, H. P. A. Mercier and G. J. Schrobilgen, *Inorg. Chem.*, 2011, **49**, 12359. g) D. S. Brock, H. P. A. Mercier and G. J. Schrobilgen, *J. Am. Chem. Soc.*, 2013, **135**, 5089; h) J. R. Debackere, H. P. A. Mercier and G. J. Schrobilgen, *J. Am. Chem. Soc.*, 2014, **136**, 3888.
14. a) G. Frenking, W. J. Gauss and D. Cremer, *J. Am. Chem. Soc.*, 1988, **110**, 8007; b) W. Koch, B. Liu and G. Frenking, *J. Chem. Phys.*, 1990, **92**, 2464; c) G. Frenking, W. Koch, F. Reichel and D. Cremer, *J. Am. Chem. Soc.*, 1990, **112**, 4240; d) A. Veldkamp and G. Frenking, *Chem. Phys. Lett.*, 1994, **226**, 11; e) C. Ó. Jiménez-Halla, I. Fernández and G. Frenking, *Angew. Chem. Int. Ed.*, 2009, **48**, 366; f) L. A. Mück, A. Y. Timoshkin, M. v. Hopffgarten and G. Frenking, *J. Am. Chem. Soc.*, 2009, **131**, 3942; g) I. Fernández and G. Frenking, *Phys. Chem. Chem. Phys.*, 2012, **14**, 14869.
15. a) N. Pérez-Peralta, R. Juárez, E. Cerpa, F. M. Bickelhaupt and G. Merino, *J. Phys. Chem. A*, 2009, **113**, 9700; b) S. Pan, M. Contreras, J. Romero, A. Reyes, P. K. Chattaraj and G. Merino, *Chem. Eur. J.*, 2013, **17**, 2322; c) S. Pan, S. Jalife, R. M. Kumar, V. Subramanian, G. Merino and P. K. Chattaraj, *ChemPhysChem*, 2013, **14**, 2511; d) S. Pan, S. Jalife, J. Romero, A. Reyes, G. Merino and P. K. Chattaraj, *Comput. Theor. Chem.*, 2013, **1021**, 62; e) S. Pan, D. Moreno, J. L. Cabellos, J. Romero, A. Reyes, G. Merino and P. K. Chattaraj, *J. Phys. Chem. A*, 2014, **118**, 487; f) M. Khatua, S. Pan and P. K. Chattaraj, *J. Chem. Phys.*, 2014, **140**, 164306; g) S. Pan, D. Moreno, J. L. Cabellos, G. Merino and P. K. Chattaraj, *ChemPhysChem*, 2014, **15**, 2618; h) S. Pan, D. Moreno, G. Merino, and P. K. Chattaraj, *ChemPhysChem*, 2014, **15**, 3554.
16. a) J. Lundell, A. Cohen and R. B. Gerber, *J. Phys. Chem. A*, 2002, **106**, 11950; b) R. B. Gerber, *Bull. Israel Chem. Soc.*, 2005, **18**, 7; c) L. Khriachtchev, M. Räsänen and R. B. Gerber, *Acc. Chem. Res.*, 2009, **42**, 183; d) U. Tsvion and R. B. Gerber, *Chem. Phys. Lett.*, **2009**, 482, 30; e) V. I. Feldman, A. V. Kobzarenko, I. A. Baranova, A. V. Danchenko, F. O. Sukhov, E. Tsvion and R. B. Gerber, *J. Chem. Phys.*, 2009, **131**, 151101.
17. a) W. Grochala, *Pol. J. Chem.*, 2009, **83**, 87; b) J. F. Lockyear, K. Douglas, S. D. Price, M. Karwowska, K. J. Fijałkowski, W. Grochala, M. Remeš, J. Roithová and D. Schröder, *J. Phys. Chem. Lett.*, 2010, **1**, 358; c) D. Kurzydłowski, P. Ejgierd-Zaleski, W. Grochala and R. Hoffmann, *Inorg. Chem.*, 2011, **50**, 3832; d) W. Grochala, *Phys. Chem. Chem. Phys.*, 2012, **14**, 14860.
18. a) P. Antoniotti, N. Bronzolino and F. Grandinetti, *J. Phys. Chem. A*, 2003, **107**, 2974; b) S. Borocci, N. Bronzolino and F. Grandinetti, *Chem. Eur. J.*, 2006, **12**, 5033; c) F. Grandinetti, *Int. J. Mass Spectrom.*, 2004, **237**, 243; d) S. Borocci, N. Bronzolino and F. Grandinetti, *Chem. Phys. Lett.*, 2005, **406**, 179; e) P. Antoniotti, E. Bottizzo, L. Operti, R. Rabezzana, S. Borocci and F. Grandinetti, *J. Phys. Chem. Lett.*, 2010, **1**, 2006; f) L. Operti, R. Rabezzana, F. Turco, S. Borocci, M. Giordani and F. Grandinetti, *Chem. Eur. J.*, 2011, **17**, 10682.
19. a) T. Jayasekharan and T. K. Ghanty, *J. Chem. Phys.*, 2006, **124**, 164309; b) T. Jayasekharan and T. K. Ghanty, *J. Chem. Phys.*, 2007, **127**, 114314; c) T. Jayasekharan and T. K. Ghanty, *J. Chem. Phys.*, 2008, **128**, 144314; d) T. Jayasekharan and T. K.

- Ghanty, *J. Chem. Phys.*, 2008, **129**, 184302; e) A. Sirohiwal, D. Manna, A. Ghosh, T. Jayasekharan and T. K. Ghanty, *J. Phys. Chem. A*, 2013, **117**, 10772; f) D. Manna, A. Ghosh and T. K. Ghanty, *J. Phys. Chem. A*, 2013, **117**, 14282; g) A. Ghosh, D. Manna and T. K. Ghanty, *J. Phys. Chem. A*, 2014, dx.doi.org/10.1021/jp5042266.
20. a) J. V. Wijngaarden and W. Jäger, *J. Chem. Phys.*, 2001, **115**, 6504; b) A. K. Dham, F. R. McCourt and A. S. Dickinson, *J. Chem. Phys.*, 2007, **127**, 054302; c) J. Han, D. Philen and M. C. Heaven, *J. Chem. Phys.*, 2006, **124**, 054314.
21. K. O. Christe, *Chem. Commun.*, 2013, **49**, 4588.
22. J. F. Lehmann, H. Mercier and G. J. Schrobilgen, *Coord. Chem. Rev.*, 2002, **233**, 1.
23. W. Grochala, *Chem. Soc. Rev.*, 2007, **36**, 1632.
24. M. Tramšek and B. Žemva, *Acta Chim. Slov.*, 2006, **53**, 105.
25. G. J. Schrobilgen and D. S. Brock, *Annu. Rep. Prog. Chem., Sect. A: Inorg. Chem.*, 2013, **109**, 101.
26. D. Holtz and J. L. Beauchamp, *Science*, 1971, **173**, 1237.
27. a) L. J. Turbini, R. E. Aikman and R. J. Lagow, *J. Am. Chem. Soc.*, 1979, **101**, 5833; b) D. Naumann and W. T. Tyrra, *J. Chem. Soc., Chem. Commun.*, 1989, 47; c) H. J. Frohn and S. Jakobs, *J. Chem. Soc., Chem. Commun.*, 1989, 625; d) H. J. Frohn, S. Jacobs and G. Henkel, *Angew. Chem., Int. Ed.*, 1989, **28**, 1506.
28. a) H.-J. Frohn and V. Bardin, *Chem. Commun.*, 1999, **10**, 919; b) H.-J. Frohn and V. V. Bardin, *Organometallics*, 2001, **20**, 4750; c) V. K. Brel, N. S. Pirkuliev and N. S. Zefirov, *Russ. Chem. Rev.*, 2001, **70**, 231; d) H.-J. Frohn and V. V. Bardin, *Chem. Commun.* 2003, **18**, 2352; e) H. J. Frohn and V. V. Bardin, *Eur. J. Inorg. Chem.*, 2006, **2006**, 3948; f) H.-J. Frohn, V. Bilir and U. Westphal, *Inorg. Chem.*, 2012, **51**, 11251; g) C. Goedecke, R. Sitt and G. Frenking, *Inorg. Chem.*, 2012, **51**, 11259; h) V. Bilir and H.-J. Frohn, *Acta Chim. Slovenica*, 2013, **60**, 505.
29. a) T. Arppe, L. Khriachtchev, A. Lignell, A. V. Domanskaya and M. Räsänen, *Inorg. Chem.*, 2012, **51**, 4398; b) L. Khriachtchev, H. Tanskanen, J. Lundell, M. Pettersson, H. Kiljunen and M. Räsänen, *J. Am. Chem. Soc.* 2003, **125**, 4696; c) L. Khriachtchev, A. Domanskaya, J. Lundell, A. Akimov, M. Räsänen and E. Misochko, *J. Phys. Chem. A*, 2010, **114**, 4181; d) L. Khriachtchev, A. Lignell, H. Tanskanen, J. Lundell, H. Kiljunen and M. Räsänen, *J. Phys. Chem. A*, 2006, **110**, 11876.
30. a) C. C. Lovallo and M. Klobukowski, *Int. J. Quantum Chem.*, 2002, **90**, 1099; b) S. Semenov and Y. F. Sigolaev, *Russ. J. Org. Chem.*, 2004, **40**, 1757; c) S. A. C. McDowell, *J. Chem. Phys.* 2004, **120**, 9077; d) J. Baker, P. W. Fowler, A. Soncini and M. Lillington, *J. Chem. Phys.*, 2005, **123**, 174309; e) A. Fitzsimmons and M. Klobukowski, *Theor. Chem. Acc.*, 2013, **132**, 1; f) M. Zhang and L. Sheng, *J. Chem. Phys.*, 2013, **138**, 114301.
31. R. Cipollini and F. Grandinetti, *J. Chem. Soc., Chem. Commun.*, 1995, **7**, 773.
32. A. Cunje, V. Baranov, Y. Ling, A. Hopkinson and D. Bohme, *J. Phys. Chem. A*, 2001, **105**, 11073.
33. J. Lundell, J. Panek and Z. Latajka, *Chem. Phys. Lett.*, 2001, **348**, 147.
34. P. Antoniotti, E. Bottizzo, L. Operti, R. Rabezzana, S. Borocci and F. Grandinetti, *J. Phys. Chem. Lett.*, 2010, **1**, 2006.
35. S. Borocci, M. Giordani and F. Grandinetti, *J. Phys. Chem. A*, 2014, **118**, 3326.
36. S. Yockel, A. Garg and A. K. Wilson, *Chem. Phys. Lett.*, 2005, **411**, 91.
37. C. Møller and M. S. Plesset, *Phys. Rev.*, 1934, **46**, 618.

38. a) F. Weigend and R. Ahlrichs, *Phys. Chem. Chem. Phys.*, 2005, **7**, 3297; b) F. Weigend, *Phys. Chem. Chem. Phys.*, 2006, **8**, 1057.
39. Gaussian 09, Revision A.1, M. J. Frisch, et al. Gaussian, Inc., Wallingford CT, 2009.
40. a) B. Metz, H. Stoll and M. Dolg, *J. Chem. Phys.*, 2000, **113**, 2563; b) K. A. Peterson, D. Figgen, E. Goll, H. Stoll and M. Dolg, *J. Chem. Phys.*, 2003, **119**, 11113.
41. J. A. Pople, M. Head-Gordon and K. Raghavachari, *J. Chem. Phys.*, 1987, **87**, 5968.
42. R. F. W. Bader, *Atoms in Molecules: A Quantum Theory*; Oxford University Press: Oxford, 1990.
43. T. Lu and F. W. Chen, *J. Comput. Chem.*, 2012, **33**, 580.
44. a) S. Huzinaga and B. Miguel, *Chem. Phys. Lett.*, 1990, **175**, 289; b) S. Huzinaga and M. Klobukowski, *Chem. Phys. Lett.*, 1993, **212**, 260.
45. W. Zou, D. Nori-Shargh and J. E. Boggs, *J. Phys. Chem. A*, 2012, **117**, 207.
46. a) K. Morokuma, *Acc. Chem. Res.*, 1977, **10**, 294; b) T. Ziegler, A. Rauk, *Theor. Chim. Acta* 1977, **46**, 1; c) T. Ziegler, A. Rauk, E. J. Baerends, *Theor. Chim. Acta*, 1977, **43**, 261; d) M. von Hopffgarten, G. Frenking, *Wiley Interdiscip. Rev. Comput. Mol. Sci.*, 2012, **2**, 43.
47. a) Y. Zhang and W. Yang, *Phys. Rev. Lett.*, 1998, **80**, 890; b) S. Grimme, J. Antony, S. Ehrlich and H. Krieg, *J. Chem. Phys.*, 2010, **132**, 154104.
48. E. Van Lenthe and E. J. Baerends, *J. Comput. Chem.*, 2003, **24**, 1142.
49. a) ADF2013.01, E. J. Baerends, T. Ziegler, J. Autschbach, D. Bashford, A. Bérces, F. M. Bickelhaupt, C. Bo, P. M. Boerrigter, L. Cavallo, D. P. Chong, L. Deng, R. M. Dickson, D. E. Ellis, M. v. Faassen, L. Fan, T. H. Fischer, C. F. Guerra, A. Ghysels, A. Giammona, S. J. A. v. Gisbergen, A. W. Götz, J. A. Groeneveld, O. V. Gritsenko, M. Gruning, S. Gusarov, F. E. Harris, P. v. d. Hoek, C. R. Jacob, H. Jacobsen, L. Jensen, J. W. Kaminski, G. v. Kessel, F. Kootstra, A. Kovalenko, M. V. Krykunov, E. v. Lenthe, D. A. McCormack, A. Michalak, M. Mitoraj, J. Neugebauer, V. P. Nicu, L. Noodleman, V. P. Osinga, S. Patchkovskii, P. H. T. Philipsen, D. Post, C. C. Pye, W. Ravenek, J. I. Rodríguez, P. Ros, P. R. T. Schipper, G. Schreckenbach, J. S. Seldenthuis, M. Seth, J. G. Snijders, M. Solà, M. Swart, D. Swerhone, G. t. Velde, P. Vernooijs, L. Versluis, L. Visscher, O. Visser, F. Wang, T. A. Wesolowski, E. M. v. Wezenbeek, G. Wiesenekker, S. K. Wolff, T. K. Woo and A. L. Yakovlev, SCM, Theoretical Chemistry, Vrije Universiteit, Amsterdam, The Netherlands, 2013; b) G. te Velde, F. M. Bickelhaupt, E. J. Baerends, C. F. Guerra, S. J. A. Van Gisbergen, J. G. Snijders and T. Ziegler, *J. Comput. Chem.*, 2001, **22**, 931.
50. a) E. van Lenthe, A. Ehlers and E. J. Baerends, *J. Chem. Phys.*, 1999, **110**, 8943; b) E. van Lenthe, E. J. Baerends and J. G. Snijders, *J. Chem. Phys.*, 1993, **99**, 4597; c) E. van Lenthe, E. J. Baerends and J. G. Snijders, *J. Chem. Phys.*, 1994, **101**, 9783; d) E. van Lenthe, J. G. Snijders and E. J. Baerends, *J. Chem. Phys.*, 1996, **105**, 6505; e) E. van Lenthe, R. vanLeeuwen, E. J. Baerends and J. G. Snijders, *Int. J. Quantum Chem.*, 1996, **57**, 281.
51. T.-H. Li, Y.-L. Liu, R.-J. Lin, T.-Y. Yeh, W.-P. Hu, *Chem. Phys. Lett.* 2007, **434**, 38.
52. B. Cordero, V. Gómez, A. E. Platero-Prats, M. Revés, J. Echeverría, E. Cremades, F. Barragán and S. Alvarez, *Dalton Trans.*, 2008, **21**, 2832.
53. P. Pykkö and M. Atsumi, *Chem. Eur. J.*, 2009, **15**, 12770.
54. a) J. Cioslowski and S. T. Mixon, *Can. J. Chem.*, 1992, **70**, 443; b) J. Cioslowski and S. T. Mixon, *J. Am. Chem. Soc.*, 1992, **114**, 4382; c) A. Haaland, D. J. Shorokhov and N.

- V. Tverdova, *Chem. Eur. J.*, 2004, **10**, 4416; d) A. Krapp and G. Frenking, *Chem. Eur. J.*, 2007, **13**, 8256; e) J. Poater, R. Visser, M. Solà and F. M. Bickelhaupt, *J. Org. Chem.*, 2007, **72**, 1134; f) E. Cerpa, A. Krapp, A. Vela and G. Merino, *Chem. Eur. J.*, 2008, **14**, 10232; g) E. Cerpa, A. Krapp, R. Flores-Moreno, K. J. Donald and G. Merino, *Chem. Eur. J.*, 2009, **15**, 1985; e) P. Macchi, D. M. Proserpio and A. J. Sironi, *J. Am. Chem. Soc.*, 1998, **120**, 13429; f) P. Macchi, L. Garlaschelli, S. Martinengo and A. J. Sironi, *J. Am. Chem. Soc.*, 1999, **121**, 10428; g) I. V. Novozhilova, A. V. Volkov and P. J. Coppens, *J. Am. Chem. Soc.*, 2003, **125**, 1079.
55. D. Cremer and E. Kraka, *Angew. Chem., Int. Ed.*, 1984, **23**, 627.
56. a) P. Macchi, D. M. Proserpio and A. J. Sironi, *J. Am. Chem. Soc.*, 1998, **120**, 13429; b) P. Macchi, L. Garlaschelli, S. Martinengo and A. J. Sironi, *J. Am. Chem. Soc.*, 1999, **121**, 10428; c) I. V. Novozhilova, A. V. Volkov and P. J. Coppens, *J. Am. Chem. Soc.*, 2003, **125**, 1079; d) L. J. Farrugia and H. M. Senn, *J. Phys. Chem. A*, 2010, **114**, 13418.

## Figures

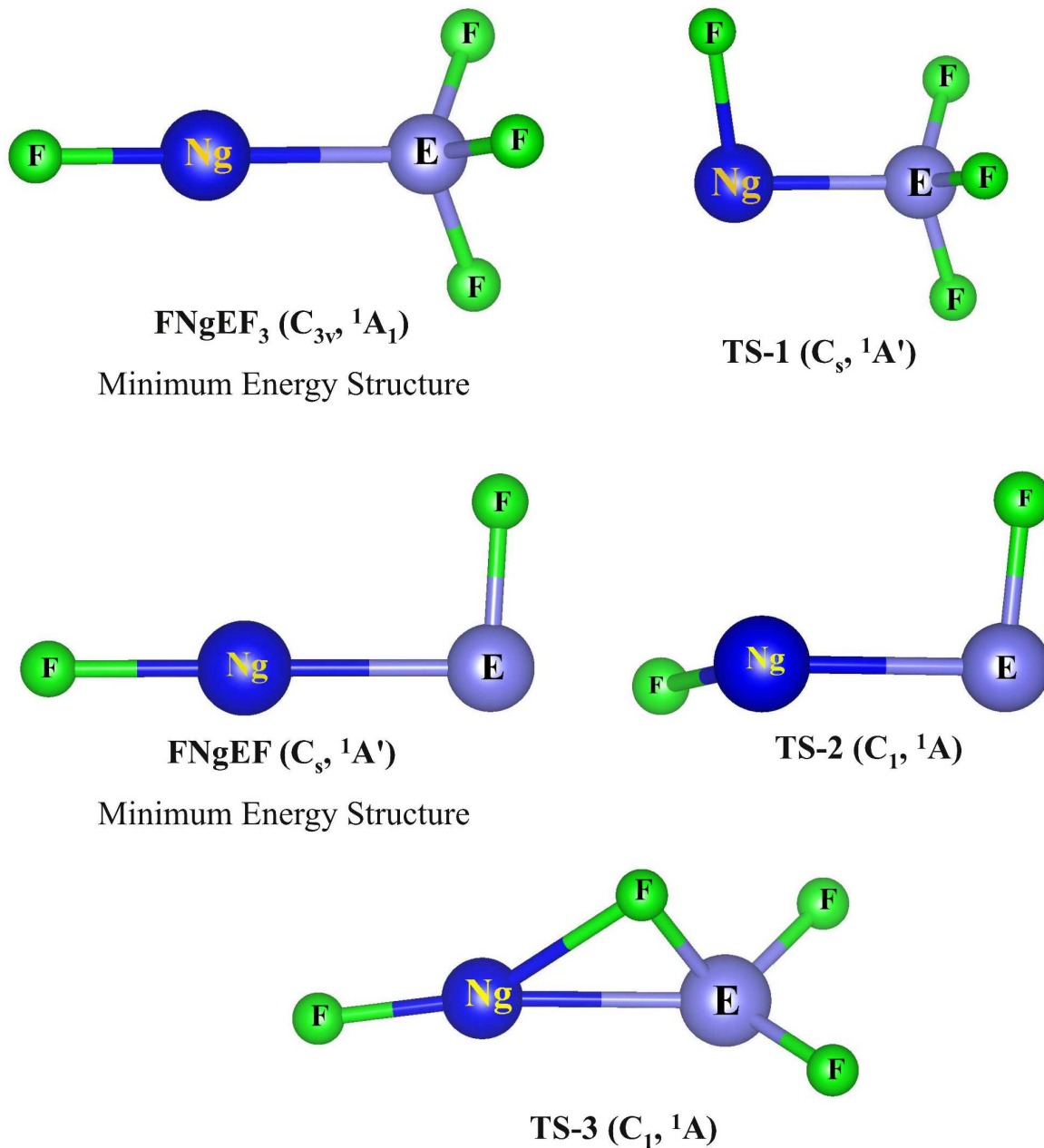


**Fig. 1** Pictorial depictions of energy minimum structures and the transition states of  $\text{FNgEF}_3$  and  $\text{FNgEF}$  clusters. Point groups along with their electronic states are given in parentheses. **TS-1** and **TS-2** are associated with the dissociation of  $\text{ENgEF}_3$  and  $\text{FNgEF}$  producing  $\text{Ng}$  and  $\text{EF}_4$  or  $\text{EF}_2$ . **TS-3** is associated with the dissociation of  $\text{ENgPbF}_3$  producing  $\text{NgF}_2$  and  $\text{PbF}_2$ .

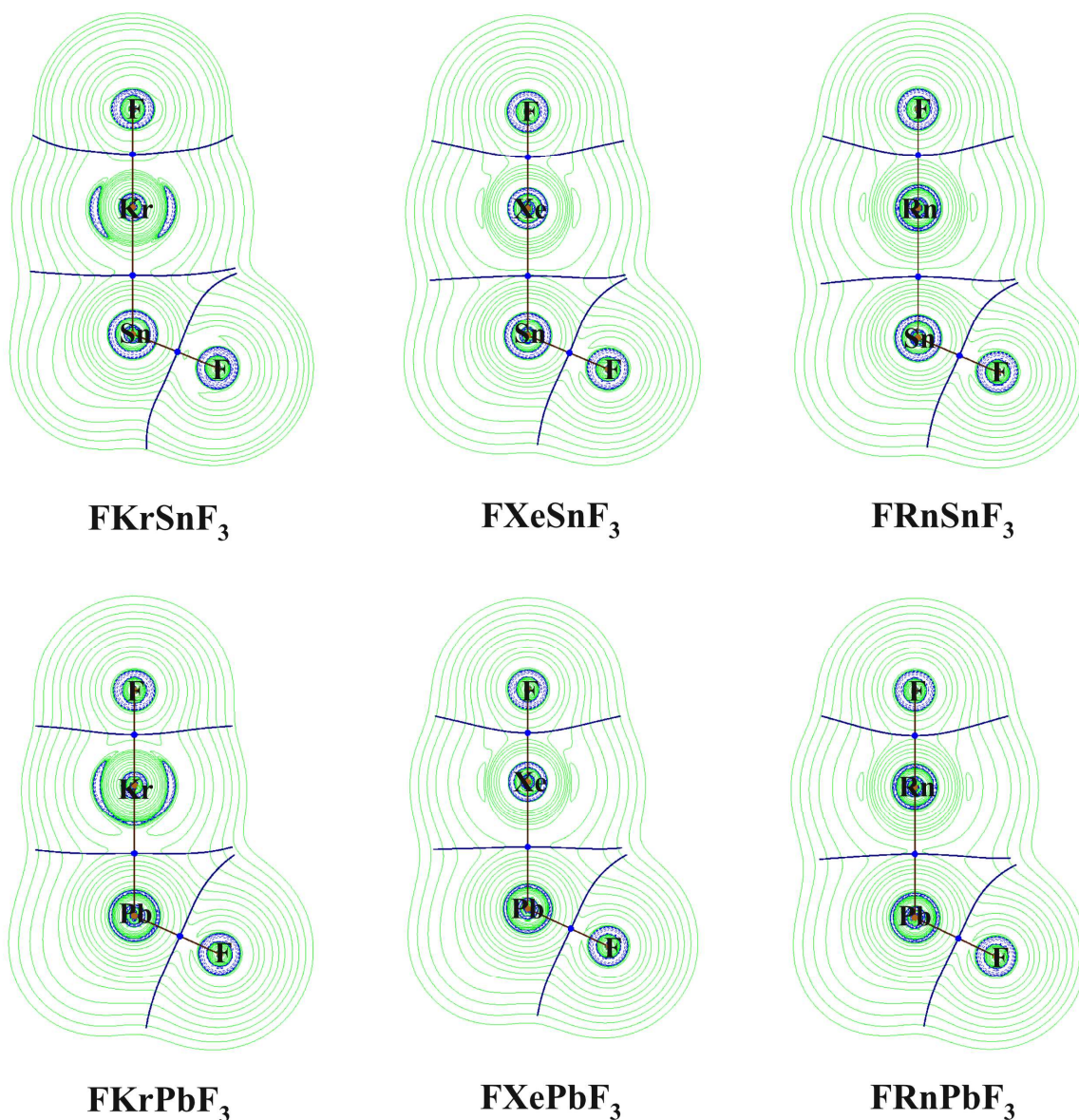


**Fig. 2** Contour plots of the Laplacian of the electron density of  $\text{FNgSnF}_3$  and  $\text{FNgPbF}_3$  clusters at a particular plane computed at the MP2/def2-TZVPPD/WTBS level. (WTBS is used for Sn, Pb, Xe and Rn; Green colored region shows the area of  $\nabla^2\rho(\mathbf{r}) > 0$  whereas blue colored region shows the area of  $\nabla^2\rho(\mathbf{r}) < 0$ )

## Tables

**Table 1.** ZPE corrected dissociation energy ( $D_0$ , kcal/mol), dissociation enthalpy ( $\Delta H$ , kcal/mol) and free energy change ( $\Delta G$ , kcal/mol) for different dissociation channels of FNgSnF<sub>3</sub> and FNgSnF clusters at the MP2/def2-TZVPPD level.

Processes	$D_0$			$\Delta H$			$\Delta G$		
	Kr	Xe	Rn	Kr	Xe	Rn	Kr	Xe	Rn
FNgSnF <sub>3</sub> → F + Ng + SnF <sub>3</sub>	7.6	31.8	46.1	8.2	32.4	46.7	-7.8	16.3	30.6
FNgSnF <sub>3</sub> → NgF <sub>2</sub> + SnF <sub>2</sub>	42.2	31.3	29.8	41.9	31.0	29.6	32.7	21.6	20.0
FNgSnF <sub>3</sub> → F <sup>-</sup> + NgSnF <sub>3</sub> <sup>+</sup>	135.5	150.9	158.5	135.9	151.3	159.0	128.0	143.3	151.1
FNgSnF <sub>3</sub> → Ng + SnF <sub>4</sub>	-105.3	-81.1	-66.7	-105.4	-81.2	-66.9	-111.3	-87.2	-72.8
$\Delta E^{\ddagger a}$	23.9	32.7	36.8						
FNgSnF → F + Ng + SnF	24.7	40.0	49.7	25.3	40.6	50.3	11.5	26.7	36.4
FNgSnF → NgF <sub>2</sub> + Sn	140.3	120.5	114.4	140.2	120.4	114.4	136.1	116.1	109.9
FNgSnF → F <sup>-</sup> + NgSnF <sup>+</sup>	95.4	106.9	113.4	95.7	107.3	113.7	87.9	99.5	106.1
FNgSnF → Ng + SnF <sub>2</sub>	-105.4	-90.1	-80.4	-105.5	-90.2	-80.5	-111.5	-96.3	-86.6
$\Delta E^{\ddagger b}$	2.9	6.9	8.7						

$\Delta E^{\ddagger a}$  is the activation barrier for the process FNgSnF<sub>3</sub> → Ng + SnF<sub>4</sub>;  $\Delta E^{\ddagger b}$  is the activation barrier for the process FNgSnF → Ng + SnF<sub>2</sub>

**Table 2.** ZPE corrected dissociation energy ( $D_0$ , kcal/mol), dissociation enthalpy ( $\Delta H$ , kcal/mol) and free energy change ( $\Delta G$ , kcal/mol) for different dissociation channels of  $\text{FNgPbF}_3$  and  $\text{FNgPbF}$  clusters at the MP2/def2-TZVPPD level.

Processes	$D_0$			$\Delta H$			$\Delta G$		
	Kr	Xe	Rn	Kr	Xe	Rn	Kr	Xe	Rn
$\text{FNgPbF}_3 \rightarrow \text{F} + \text{Ng} + \text{PbF}_3$	-0.2	23.2	38.4	0.3	23.8	39.0	-14.8	8.0	23.2
$\text{FNgPbF}_3 \rightarrow \text{NgF}_2 + \text{PbF}_2$	1.7	-10.0	-10.7	1.1	-10.5	-11.1	-6.7	-19.1	-19.8
$\text{FNgPbF}_3 \rightarrow \text{F}^- + \text{NgPbF}_3^+$	149.0	163.7	172.0	149.4	164.1	172.4	142.1	156.3	164.6
$\text{FNgPbF}_3 \rightarrow \text{Ng} + \text{PbF}_4$	-76.9	-53.5	-38.3	-77.1	-53.6	-38.5	-82.2	-59.4	-44.3
$\Delta E^{\ddagger a}$	40.5	46.6	49.9						
$\Delta E^{\ddagger b}$	-a-	13.8	10.1						
$\text{FNgPbF} \rightarrow \text{F} + \text{Ng} + \text{PbF}$	26.2	41.1	50.7	26.8	41.7	51.3	13.1	27.9	37.5
$\text{FNgPbF} \rightarrow \text{NgF}_2 + \text{Pb}$	134.2	113.9	107.7	134.0	113.8	107.6	130.1	109.7	103.3
$\text{FNgPbF} \rightarrow \text{F}^- + \text{NgPbF}^+$	92.2	103.6	110.2	92.6	103.9	110.5	84.9	96.2	102.9
$\text{FNgPbF} \rightarrow \text{Ng} + \text{PbF}_2$	-95.4	-80.5	-70.9	-95.5	-80.6	-71.1	-101.5	-86.7	-77.1
$\Delta E^{\ddagger c}$	2.2	6.0	7.8						

$\Delta E^{\ddagger a}$  is the activation barrier for the process  $\text{FNgPbF}_3 \rightarrow \text{Ng} + \text{PbF}_4$ ;  $\Delta E^{\ddagger b}$  is the activation barrier for the process  $\text{FNgPbF}_3 \rightarrow \text{NgF}_2 + \text{PbF}_2$ ;  $\Delta E^{\ddagger c}$  is the activation barrier for the process  $\text{FNgPbF} \rightarrow \text{Ng} + \text{PbF}_2$ . -a- the transition state cannot be located.



**Table 3.** NPA charge on each atomic center ( $q_k$ , au) and WBI values of F-Ng and Ng-E bonds computed at the MP2/def2-TZVPPD level.

Clusters	$q_k$			WBI		
	F(Ng)	Ng	E	F(E)	F-Ng	Ng-E
FKrSnF <sub>3</sub>	-0.81	+0.49	+2.55	-0.74	0.17	0.66
FXeSnF <sub>3</sub>	-0.82	+0.69	+2.38	-0.75	0.20	0.79
FRnSnF <sub>3</sub>	-0.83	+0.79	+2.31	-0.76	0.19	0.82
FKrSnF	-0.94	+0.23	+1.53	-0.82	0.06	0.43
FXeSnF	-0.92	+0.37	+1.37	-0.82	0.10	0.62
FRnSnF	-0.92	+0.44	+1.30	-0.82	0.10	0.70
FKrPbF <sub>3</sub>	-0.69	+0.59	+2.28	-0.73	0.25	0.60
FXePbF <sub>3</sub>	-0.74	+0.82	+2.14	-0.74	0.28	0.72
FRnPbF <sub>3</sub>	-0.77	+0.94	+2.08	-0.75	0.27	0.73
FKrPbF	-0.94	+0.20	+1.57	-0.83	0.05	0.38
FXePbF	-0.926	+0.33	+1.42	-0.83	0.09	0.57
FRnPbF	-0.928	+0.411	+1.35	-0.83	0.09	0.66

**Table 4.** Electron density descriptors (au) at the bond critical points (BCP) of F-Ng and Ng-E bonds of FN<sub>g</sub>EF<sub>3</sub> and FN<sub>g</sub>EF compounds obtained from the wave functions generated at the MP2/def2-TZVPPD/WTBS level (WTBS for Sn, Pb, Xe and Rn atoms) taking optimized geometries at the MP2/def2-TZVPPD level.

Clusters	BCP	$\rho(r_c)$	$\nabla^2\rho(r_c)$	$G(r_c)$	$V(r_c)$	$H(r_c)$	$G(r_c)/\rho(r_c)$	Class	$r_{cov}$	$r_e$
FKrSnF <sub>3</sub>	F-Kr	0.104	0.281	0.101	-0.132	-0.031	0.971	B, C	1.73 <sup>a</sup> /1.81 <sup>b</sup>	2.03
	Kr-Sn	0.061	0.081	0.037	-0.053	-0.016	0.607	C	2.55 <sup>a</sup> /2.57 <sup>b</sup>	2.62
FXeSnF <sub>3</sub>	F-Xe	0.090	0.290	0.099	-0.125	-0.026	1.100	W <sup>c</sup>	1.97 <sup>a</sup> /1.95 <sup>b</sup>	2.10
	Xe-Sn	0.054	0.041	0.024	-0.037	-0.013	0.444	C	2.79 <sup>a</sup> /2.71 <sup>b</sup>	2.76
FRnSnF <sub>3</sub>	F-Rn	0.085	0.308	0.100	-0.123	-0.023	1.176	W <sup>c</sup>	2.07 <sup>a</sup> /2.06 <sup>b</sup>	2.16
	Rn-Sn	0.053	0.030	0.021	-0.035	-0.014	0.396	C	2.89 <sup>a</sup> /2.82 <sup>b</sup>	2.83
FKrSnF	F-Kr	0.062	0.233	0.065	-0.071	-0.006	1.048	W <sup>c</sup>	1.73 <sup>a</sup> /1.81 <sup>b</sup>	2.24
	Kr-Sn	0.049	0.108	0.036	-0.046	-0.010	0.735	C	2.55 <sup>a</sup> /2.57 <sup>b</sup>	2.68
FXeSnF	F-Xe	0.065	0.245	0.072	-0.083	-0.011	1.108	W <sup>c</sup>	1.97 <sup>a</sup> /1.95 <sup>b</sup>	2.27
	Xe-Sn	0.043	0.055	0.022	-0.030	-0.008	0.512	C	2.79 <sup>a</sup> /2.71 <sup>b</sup>	2.85
FRnSnF	F-Rn	0.065	0.240	0.072	-0.085	-0.013	1.108	W <sup>c</sup>	2.07 <sup>a</sup> /2.06 <sup>b</sup>	2.31
	Rn-Sn	0.043	0.042	0.019	-0.028	-0.009	0.442	C	2.89 <sup>a</sup> /2.82 <sup>b</sup>	2.93
FKrPbF <sub>3</sub>	F-Kr	0.105	0.278	0.101	-0.132	-0.031	0.962	B, C	1.73 <sup>a</sup> /1.81 <sup>b</sup>	2.02
	Kr-Pb	0.049	0.064	0.026	-0.037	-0.011	0.531	C	2.62 <sup>a</sup> /2.61 <sup>b</sup>	2.75
FXePbF <sub>3</sub>	F-Xe	0.096	0.305	0.107	-0.137	-0.030	1.115	W <sup>c</sup>	1.97 <sup>a</sup> /1.95 <sup>b</sup>	2.07
	Xe-Pb	0.049	0.054	0.024	-0.034	-0.010	0.490	C	2.86 <sup>a</sup> /2.75 <sup>b</sup>	2.85
FRnPbF <sub>3</sub>	F-Rn	0.091	0.338	0.111	-0.137	-0.026	1.220	W <sup>c</sup>	2.07 <sup>a</sup> /2.06 <sup>b</sup>	2.12
	Rn-Pb	0.049	0.044	0.022	-0.033	-0.011	0.449	C	2.96 <sup>a</sup> /2.86 <sup>b</sup>	2.90
FKrPbF	F-Kr	0.059	0.225	0.061	-0.067	-0.006	1.034	W <sup>c</sup>	1.73 <sup>a</sup> /1.81 <sup>b</sup>	2.26
	Kr-Pb	0.047	0.117	0.037	-0.044	-0.007	0.787	C	2.62 <sup>a</sup> /2.61 <sup>b</sup>	2.80
FXePbF	F-Xe	0.064	0.241	0.070	-0.081	-0.011	1.094	W <sup>c</sup>	1.97 <sup>a</sup> /1.95 <sup>b</sup>	2.29
	Xe-Pb	0.041	0.066	0.023	-0.029	-0.006	0.561	C	2.86 <sup>a</sup> /2.75 <sup>b</sup>	2.92
FRnPbF	F-Rn	0.064	0.237	0.071	-0.083	-0.012	1.109	W <sup>c</sup>	2.07 <sup>a</sup> /2.06 <sup>b</sup>	2.32
	Rn-Pb	0.041	0.054	0.021	-0.028	-0.007	0.512	C	2.96 <sup>a</sup> /2.86 <sup>b</sup>	2.99

<sup>a</sup>the  $r_{cov}$  distance according to ref. 52 and <sup>b</sup>the  $r_{cov}$  distance according to ref. 53.

**Table 5.** EDA results of FNgSnF<sub>3</sub> and FNgSnF compounds (Ng = Kr-Rn) studied at the revPBE-D3/TZ2P//MP2/def2-TZVPPD level.

Systems	Fragments	$\Delta E_{\text{int}}$	$\Delta E_{\text{pauli}}$	$\Delta E_{\text{elstat}}$	$\Delta E_{\text{orb}}$	$\Delta E_{\text{disp}}$
FKrSnF <sub>3</sub>	F <sup>-</sup> + [KrSnF <sub>3</sub> ] <sup>+</sup>	-167.77	120.22	-186.20 (64.7%)	-101.63 (35.3%)	-0.15 (0.1%)
	[FKr] + [SnF <sub>3</sub> ]	-37.48	127.97	-40.66 (24.6%)	-123.88 (74.9%)	-0.91 (0.6%)
FXeSnF <sub>3</sub>	F <sup>-</sup> + [XeSnF <sub>3</sub> ] <sup>+</sup>	-177.17	140.58	-211.40 (66.5%)	-106.23 (33.4%)	-0.12 (0.0%)
	[FXe] + [SnF <sub>3</sub> ]	-42.82	149.56	-50.16 (26.1%)	-141.19 (73.4%)	-1.03 (0.5%)
FRnSnF <sub>3</sub>	F <sup>-</sup> + [RnSnF <sub>3</sub> ] <sup>+</sup>	-181.02	134.62	-216.61 (68.6%)	-98.92 (31.3%)	-0.11 (0.0%)
	[FRn] + [SnF <sub>3</sub> ]	-45.56	153.69	-53.76 (27.0%)	-144.35 (72.4%)	-1.14 (0.6%)
FKrSnF	F <sup>-</sup> + [KrSnF] <sup>+</sup>	-122.91	61.39	-127.74 (69.3%)	-56.37 (30.6%)	-0.19 (0.1%)
	[FKr] <sup>-</sup> + [SnF] <sup>+</sup>	-134.15	70.62	-126.23 (61.6%)	-77.87 (38.0%)	-0.68 (0.3%)
	[FKr] + [SnF]	-47.87	143.33	-41.87 (21.9%)	-148.65 (77.7%)	-0.68 (0.4%)
FXeSnF	F <sup>-</sup> + [XeSnF] <sup>+</sup>	-130.19	87.89	-149.70 (68.6%)	-68.26 (31.3%)	-0.13 (0.1%)
	[FXe] <sup>-</sup> + [SnF] <sup>+</sup>	-142.74	90.53	-144.64 (62.0%)	-87.89 (37.7%)	-0.75 (0.3%)
	[FXe] + [SnF]	-47.91	153.80	-46.51 (23.1%)	-154.46 (76.6%)	-0.75 (0.4%)
FRnSnF	F <sup>-</sup> + [RnSnF] <sup>+</sup>	-133.38	91.46	-157.14 (69.9%)	-67.57 (30.1%)	-0.13 (0.1%)
	[FRn] <sup>-</sup> + [SnF] <sup>+</sup>	-146.06	103.99	-156.12 (62.4%)	-93.09 (37.2%)	-0.84 (0.3%)
	[FRn] + [SnF]	-47.91	156.75	-49.00 (24.0%)	-153.92 (75.5%)	-0.84 (0.4%)

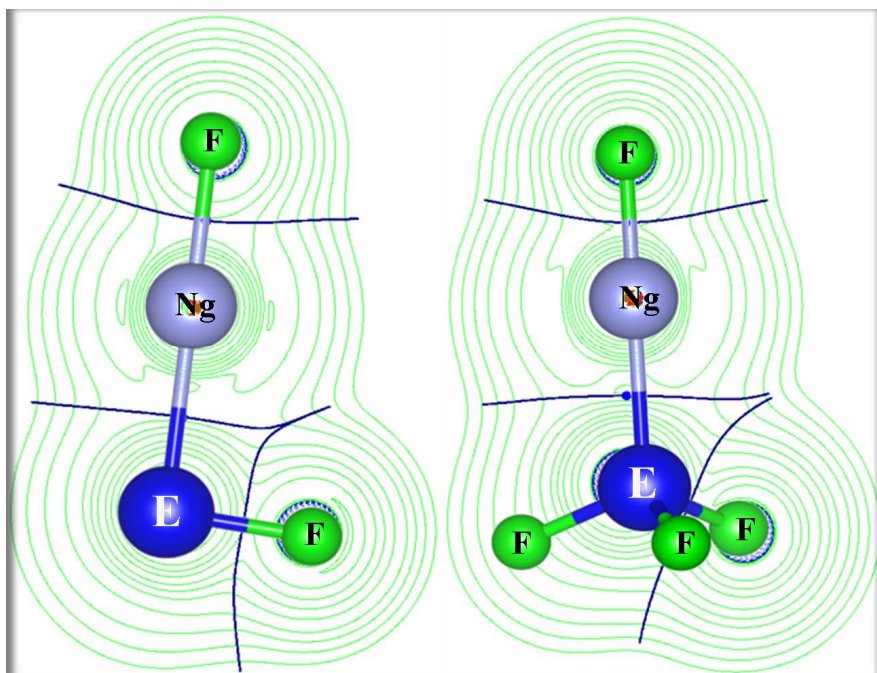
(The percentage values within the parentheses show the contribution towards the total attractive interaction  $\Delta E_{\text{elstat}} + \Delta E_{\text{orb}} + \Delta E_{\text{disp}}$ )

**Table 6.** EDA results of FNgPbF<sub>3</sub> and FNgPbF compounds (Ng = Kr-Rn) studied at the revPBE-D3/TZ2P//MP2/def2-TZVPPD level.

Systems	Fragments	$\Delta E_{\text{int}}$	$\Delta E_{\text{pauli}}$	$\Delta E_{\text{elstat}}$	$\Delta E_{\text{orb}}$	$\Delta E_{\text{disp}}$
FKrPbF <sub>3</sub>	F <sup>-</sup> + [KrPbF <sub>3</sub> ] <sup>+</sup>	-179.64	123.72	-181.40 (59.8%)	-121.81 (40.2%)	-0.15 (0.0%)
	[FKr] + [PbF <sub>3</sub> ]	-26.05	64.24	-15.55 (17.2%)	-73.97 (81.9%)	-0.77 (0.9%)
FXePbF <sub>3</sub>	F <sup>-</sup> + [XePbF <sub>3</sub> ] <sup>+</sup>	-187.87	157.28	-219.76 (63.7%)	-125.28 (36.3%)	-0.12 (0.0%)
	[FXe] + [PbF <sub>3</sub> ]	-32.40	100.16	-30.25 (22.8%)	-101.43 (76.5%)	-0.88 (0.7%)
FRnPbF <sub>3</sub>	F <sup>-</sup> + [RnPbF <sub>3</sub> ] <sup>+</sup>	-191.48	151.34	-227.03 (66.2%)	-115.67 (33.7%)	-0.11 (0.0%)
	[FRn] + [PbF <sub>3</sub> ]	-35.59	112.43	-36.54 (24.7%)	-110.49 (74.6%)	-0.99 (0.7%)
FKrPbF	F <sup>-</sup> + [KrPbF] <sup>+</sup>	-119.14	57.38	-122.02 (69.1%)	-54.30 (30.8%)	-0.19 (0.1%)
	[FKr] <sup>-</sup> + [PbF] <sup>+</sup>	-128.67	61.35	-119.92 (63.1%)	-69.46 (36.6%)	-0.64 (0.3%)
	[FKr] + [PbF]	-48.64	125.40	-35.41 (20.3%)	-137.99 (79.3%)	-0.64 (0.4%)
FXePbF	F <sup>-</sup> + [XePbF] <sup>+</sup>	-126.37	84.48	-144.40 (68.5%)	-66.31 (31.4%)	-0.14 (0.1%)
	[FXe] <sup>-</sup> + [PbF] <sup>+</sup>	-136.98	83.06	-140.58 (63.9%)	-78.73 (35.8%)	-0.72 (0.3%)
	[FXe] + [PbF]	-47.99	138.35	-40.87 (21.9%)	-144.76 (77.7%)	-0.72 (0.4%)
FRnPbF	F <sup>-</sup> + [RnPbF] <sup>+</sup>	-129.87	88.83	-152.45 (69.7%)	-66.12 (30.2%)	-0.13 (0.1%)
	[FRn] <sup>-</sup> + [PbF] <sup>+</sup>	-140.37	98.59	-154.30 (64.6%)	-83.83 (35.1%)	-0.83 (0.3%)
	[FRn] + [PbF]	-47.84	143.74	-45.03 (23.5%)	-145.71 (76.1%)	-0.83 (0.4%)

(The percentage values within the parentheses show the contribution towards the total attractive interaction  $\Delta E_{\text{elstat}} + \Delta E_{\text{orb}} + \Delta E_{\text{disp}}$ )

## Graphical Abstract



The metastable FNgEF and FNgEF<sub>3</sub> (E = Sn, Pb; Ng = Kr-Rn) are the first reported neutral compounds possessing Ng-Sn and Ng-Pb covalent bonds.